Metallurgist, Vol. 57, Nos. 11–12, March, 2014 (Russian Original Nos. 11–12, November–December, 2013)

EFFECT OF THE GEOMETRY OF AN INGOT ON ITS CHEMICAL HETEROGENEITY. PART I

V. S. Dub, A. N. Romashkin, A. N. Mal'ginov, I. A. Ivanov, and D. S. Tolstykh

UDC 669-412:620.192.43

Certain general trends in the radial and axial distribution of segregates in forging ingots are identified based on computer modeling and a generalization of data from studies of chemical heterogeneity in such ingots. Recommendations are developed on optimizing the geometry of forging ingots to minimize this heterogeneity.
Keywords: *ingot, technology, casting, heterogeneity, liquation, segregation, solidification rate.*

The properties of finished metal products obtained from forging ingots can vary widely as a result of chemical heterogeneity of the ingot. The coarser manifestations of this heterogeneity (such as nonaxial stringers) can lead to problems in the fabrication of important products and can sometimes necessitate rejection of the finished product or the semifinished product.

The development of chemical heterogeneity in an ingot depends on the kinetic features of its solidification, which in turn depend on the ingot's dimensions and configuration.

The ingots that are least affected by chemical heterogeneity are those that solidify as quickly as possible, i.e., ingots which have the largest specific (per unit of mass) cooling surface: ingots with a high (long rods) or ultralow (thin disks) ratio of height to diameter *h*/*d* (Fig. 1) – ingots with a more complex surface. However, such ingots have a limited range of applications.

Although the manner in which chemical heterogeneity develops in ingots has been the subject of many investigations, finding an ingot geometry that will be optimum from the standpoint of increasing the number of possible uses of ingots while simultaneously minimizing their chemical heterogeneity remains an important problem.

In light of the foregoing, in this article we offer recommendations on improving the geometry of forging ingots to minimize their chemical heterogeneity while maintaining their existing range of applications.

In the first part of the article, the chemical heterogeneity of ingots is described qualitatively and an attempt is made to interpret the results which have been obtained in practice. The second part presents results obtained by using computer modeling to study of the effect of the geometry of ingots on their chemical heterogeneity. General technical recommendations are given on optimizing the geometry of ingots in order to alleviate their chemical heterogeneity.

Part 1. QUALITATIVE DESCRIPTION OF THE CHEMICAL HETEROGENEITY OF AN INGOT

A generalization of results obtained more than 50 years ago at the Central Research Institute of Machine Building Technology (TsNIITMASh) from study of the chemical heterogeneity of forging ingots shows that the content of segregates in the bottom part of an ingot generally decreases over the ingot's radius from the periphery to the center; the degree of segregation varies in the ingot's middle part (depending on the geometry of the ingot and the composition of the steel being cast) but increases substantially in the region under the hot top; here, the content of impurities in the surface layers of the ingot usually increases relatively little (by 10–15 rel.%) from the bottom to the top of the ingot (Fig. 2).

Scientific and Production Association Central Research Institute of Machine Building Technology (NPO TsNIITMASh), Translated from Metallurg, No. 11, pp. 45–52, November, 2013. Original article submitted February 18, 2013.

0026-0894/14/1112-0987

The concentration of impurities in the axial part of the ingot usually decreases from the convex base to a plane located at roughly (0.2–0.3)h and then monotonically increases (Fig. 3). The difference between the lowest and highest concentrations can reach hundreds of percent over the ingot's height.

Such a pattern of change in impurity content is related to aspects of the impurities' distribution between the liquid and solid phases during solidification and can be explained as follows. In accordance with the law that governs the distribution of impurities during the solidification of iron-based melts, the solid phase has a lower impurity content than the initial melt as the solid phase is being formed. The difference in the concentrations of impurities in the liquid and solid metal depends on the cooling rate and can change from zero to the maximum value corresponding to the equilibrium constitution diagram. Here, the value of the coefficient that characterizes the impurity distribution changes from unity to the equilibrium value (Fig. 4). The lower the rate of solidification, the closer the system comes to equilibrium and, thus, the greater the difference between the impurity contents of the liquid and solid metal.

During the formation of the surface region of the ingot (particularly in the bottom one-quarter of the ingot, where the cooling surface is most developed), the rate of solidification is relatively high and the degree of segregation in the liquid is low. Thus, the concentration of impurities in this part of the ingot differs little from the impurity content of the metal as it was initially being cast. The rate of solidification decreases going away from the surface, the distribution coefficient also decreases, and fewer impurities thus end up in the solid metal. As a result, the concentration of impurities also decreases from the periphery of the ingot to its center. These patterns persist until conditions are such that – despite the low distribution coefficient – the impurity content of the liquid phase reaches a value at which the volume of the solid phase formed during the next stage ends up having more impurities than the volume formed in the previous stage. After this point, the impurity content of the solid phase begins to increase and will continue to do so until solidification ends.

To demonstrate the validity of the above interpretation of events, we calculated the impurity contents seen with constant and variable values for the distribution coefficient. It should be pointed out that this calculation is not a valid tool for studying processes which take place during the solidification of microscopic volumes of the metal. It is being used here only to describe the solidification of macroscopic volumes of metal, when the distribution coefficient can vary significantly.

We examined the Sheil crystallization model [7]. In this model, no diffusion of impurities takes place in the solid phase, while the composition of the metal undergoes instantaneous averaging in the liquid phase. In accordance with the model, the concentration of impurities in the solid phase can be calculated from the expression

$$C_{S(i)} = k_i C_{(i)} / [1 + (\mathrm{k} - 1)\eta_S], \tag{1}$$

where $C_{S(i)}$ is the concentration of the ith impurity in the solid phase, %; k_i is the equilibrium value of the distribution coefficient for the ith impurity; $C_{(i)}$ is the initial concentration of the impurity in the melt, %; and η_S is the solid-phase fraction.

The value of $C_{S(i)}$ was calculated for the case $k_i = 0.25$ (the equilibrium value for the coefficient that describes the distribution of carbon in iron) and $k = f(v_{\text{solid}})$. In the last case, the quantity k is calculated in relation to solidification rate by means of the formula proposed by Prim, Burton, and Clichter in [8]:

$$k = k_0 / [k_0 + (1 - k_0)\exp(-v_{\text{solid}}\delta / d)], \tag{2}$$

where d is the diffusion coefficient, m^2/sec (it has a value on the order of $(1–6)\cdot 10^{-5}$ m^2/sec); k_0 is the equilibrium distribution coefficient; v_{solid} is the rate of advance of the phase boundary, m/sec; δ is the thickness of the diffusion layer, m (this quantity changes in relation to the rate of advance of the boundary, ranging from 10^{-5} (very high rate) to 10^{-3} m (natural convection)).

The results obtained from determining the progressive movement of the low point of the liquid-metal bath (in essence, the vertical rate of crystallization) during the solidification of steel ingots in ingot molds show that the rate of solidification of steel ingots changes roughly from 0.001 to 0.02–0.03 cm/sec over 10–100% of the height of the ingot's body. The rate changes in accordance with a parabolic law, and it reaches its maximum at the 70–90% level (Fig. 5).

However, the solidification rate is significantly higher during the initial stages: for example, the first several centimeters of the skin of the ingot are formed at rates in the range 0.01–0.10 cm/sec and the rest of the ingot – roughly 0.5 m of

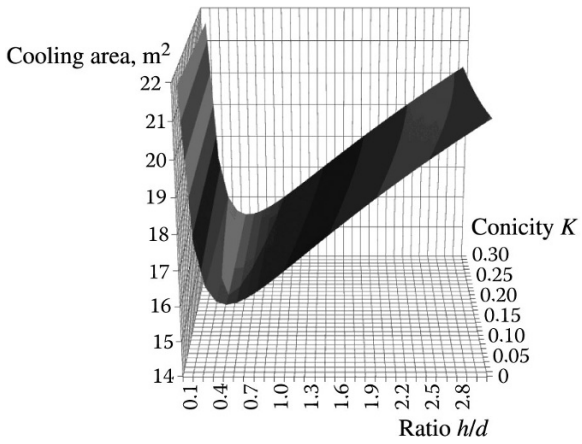

Fig. 1. Dependence of the area of the cooling surface (the sum of the areas of the lateral and lower end surfaces) of a smooth (unconstrained) big-end-up 70-ton ingot on the ratio h/d and the conicity.

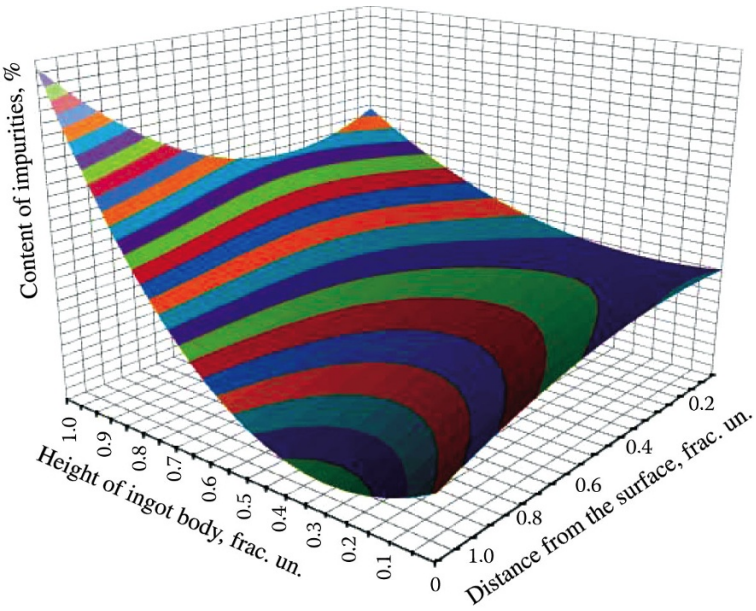

Fig. 2. Overall pattern of segregate distribution in an ingot in the axial and radial directions (for ingots whose geometry ensures the existence of the conditions necessary for directional solidification and prevents the formation of nonaxial stringers).

its thickness – is formed at rates in the range 0.001–0.01 cm/sec. This conforms to the well-known square-root law: the thickness of the solidifying skin is approximately proportional to solidification time to a power of 0.5:

$$\delta = k_{\text{solid}}\tau^{0.5}, \tag{3}$$

where δ is the thickness of the solidified skin, mm; k_{solid} is the solidification coefficient, mm/sec$^{0.5}$ (in practice, this coefficient also changes little for metal in an ingot mold that undergoes normal cooling – it has a value within the range 2.8–3.2 mm/sec$^{0.5}$); and τ is solidification time, sec.

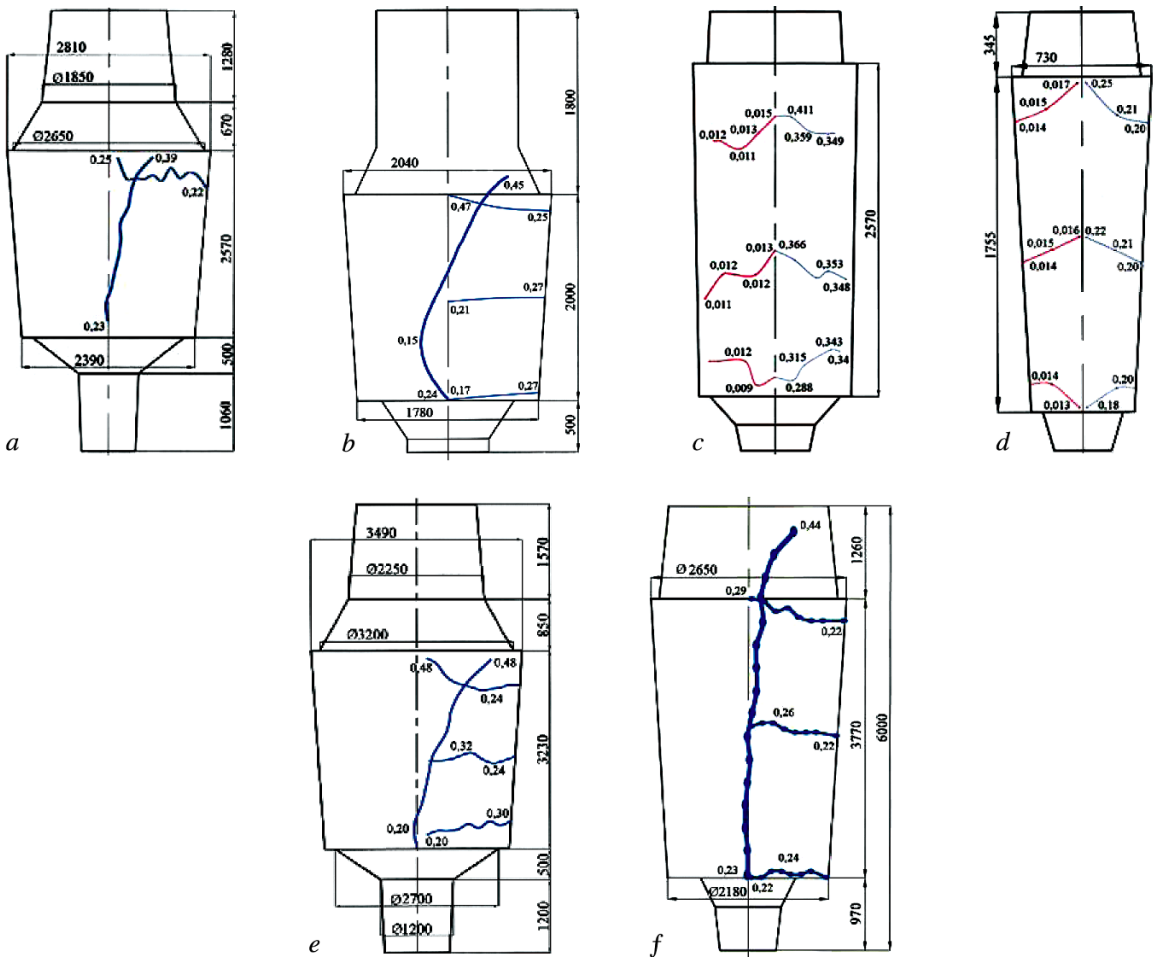

Fig. 3. Radial and axial distributions of carbon in ingots of different weights: *a*) 142-ton ingot, steel 25KhN3MFA [1]; *b*) 57-ton ingot, steel 25Kh2NMFA [2]; *c*) 32.6-ton ingot, steel 35KhN3MFA [3]; *d*) 6.57-ton ingot, steel 20 [4, 5]; *e*) 290-ton ingot (data from TsNIITMASh); *f*) 180-ton ingot of steel 5NiCrMoV [6].

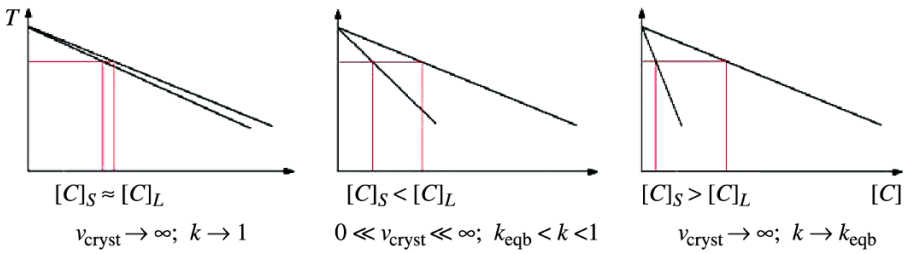

Fig. 4. Change in the impurity distribution between the liquid and solid phases as solidification of the ingot proceeds.

The existence of such high solidification rates in the surface region of the ingot shows that the curve which describes the dependence of the rate of crystallization on ingot height should be sinusoidal and have its first and second maxima at the points $h = 0$ and $h = 70–90\%$ (Fig. 6).

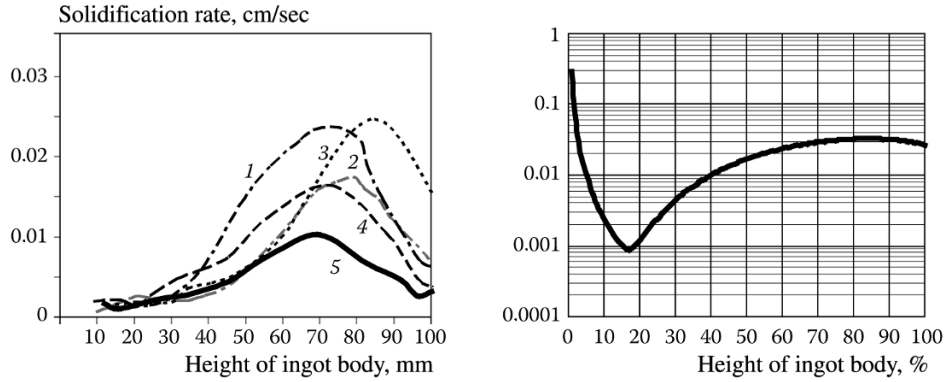

Fig. 5. Change in the rate of advance of the low point of the liquid-metal bath over the height of the ingot: *a*) results of computer modeling (*1* and *2* – for two 20-ton ingots of steel with 9% Cr – 1% Mo [9]; *3* – for a 110-ton ingot for which the ratio of the average diameters of the hot top and the ingot body was equal to 0.71; the ingot was made of steel with 3.5% Ni–Cr–Mo–V [10]; *4* – for two 135-ton ingots of steel with 3.5% Ni–Cr–Mo–V [10]; *5* – for a 110-ton ingot for which the ratio of the average diameters of the hot top and the ingot body was equal to 0.91; the ingot was made of steel with 3.5% Ni–Cr–Mo–V [10]); *b*) general path of the curve that describes the change in solidification rate over the height of the ingot.

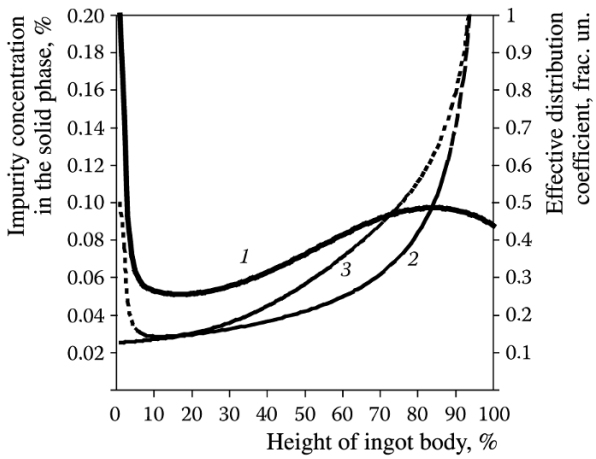

Fig. 6. Change in the effective distribution coefficient (*1*) and concentration of impurities over the height of an ingot with a constant distribution coefficient (*2*) and a distribution coefficient that depends on the content of the solid phase (*3*).

Thus, the rate at which an ingot solidifies in the vertical direction first decreases sharply, then increases somewhat, and subsequently decreases by a moderate amount at the end of the solidification process. The sharp decrease in solidification rate during the initial stages of this process is probably related to an increase in the heat resistance of the metal's solid skin. The increase seen in solidification rate in the vertical direction is connected with an increase in the specific surface for the removal of heat from the crater of liquid metal and with merging of the horizontally directed solidification fronts. Finally, the decrease in the rate of solidification which occurs during the last stages is related to the thermal effect of the hot top.

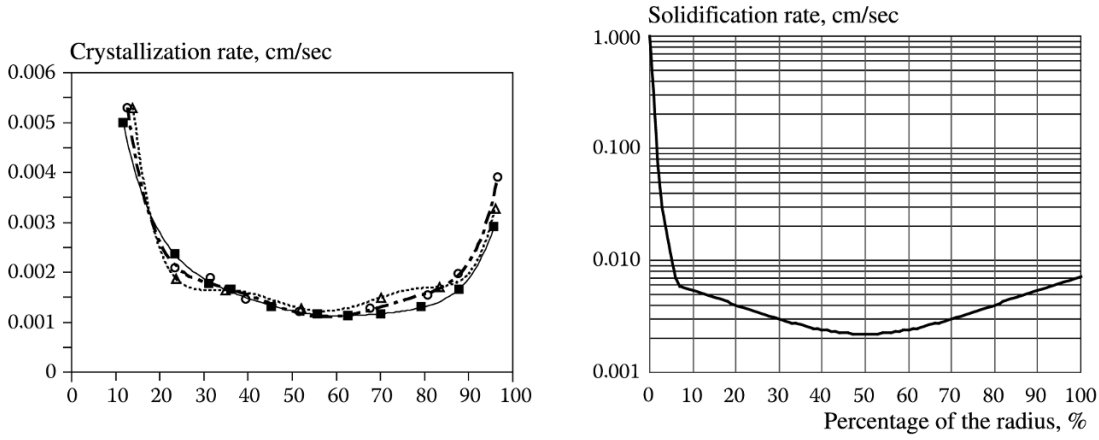

a *b*

Fig. 7. Change in the rate of growth of the solid phase in the horizontal direction: *a*) in the hot-top section for 110-ton and 135-ton ingots of a steel containing 3.5% Ni–Cr–Mo–V [12] (see Fig. 5 for the notation); *b*) general pattern of change in the rate of growth of the solid phase in the radial direction.

Figure 6 shows results obtained by calculating values of the distribution coefficient k from Eq. (2) (with $\delta = 10^{-3}$ cm and $D_C = 3 \cdot 10^{-5}$ m^2/sec – the diffusion coefficient of carbon) with allowance for the sinusoidal dependence of solidification rate on height (see Fig. 5*b*). The same figure also shows results from calculation of the impurity distribution based on Eq. (1) with k = const and $k = f(v_{\text{solid}})$. It can be seen that with a constant value for the distribution coefficient the impurity content of the solid metal increases continuously, while when $k = f(v_{\text{solid}})$ is initially decreases and only later increases. Comparison of the curves in Fig. 6 with the curves of the axial impurity distribution in Fig. 3 (to reduce the curves to the same form, one of the figures should be rotated 90° and displayed vertically) shows that the case in which k varies corresponds to the results actually obtained in practice. Thus, the interpretation offered here for the change in the chemical composition of the axial zone of the ingot over its height is proven valid.

We should once again emphasize that the functional relationship used here to characterize the dependence of the distribution coefficient on the solid-phase fraction is only a tool for demonstrating certain features of the redistribution that the impurities undergo inside the ingot: it is difficult to use the same procedure in calculations, since it would then be necessary to specify the dependence of solidification rate on skin thickness for the axial and radial directions. It would also be necessary to consider the changes in the coefficients of the equations over the height of the ingot – or at least assign values for them for the three parts of the ingot that vary significantly in the solidification conditions (the bottom and middle of the ingot and the part under the hot top).

The change in impurity content in the radial direction is of a somewhat different nature. As had already been noted, experimental results show that impurity content in the bottom part of the ingot decreases going away from its surface in the transverse direction, while it behaves differently in the middle part and increases substantially in the region under the hot top. In order to interpret the character of the change in the concentration of impurities along the ingot radius based on the above findings (for the axial distribution of segregates), we will examine the change in solidification rate in the ingot's transverse plane (Fig. 7).

It is apparent from the data in Fig. 7 that the character of the function $v_{\text{solid}} = f(R)$ is U-shaped and has a minimum at the distance (0.5–0.7)R from the surface. The range of variation of solidification rate is appreciably narrower in the horizontal direction than the vertical direction. For example, whereas it is 0.025–0.30 cm/sec at the distance (0.1–1.0)R from the surface, the range of variation is almost an order of magnitude smaller in the horizontal direction and the rate is roughly 0.005 cm/sec. It follows from this that, first of all, the dependence of solidification rate in the horizontal direction on the distance from the surface of the ingot is L-shaped. Secondly, the distribution coefficient along the ingot radius changes very little. Thus, there should also be less of a change in impurity content, and the character of its distribution can be explained by other factors.

Figure 8 shows results obtained from calculating k from Eq. (2) and calculating $C_{S(i)}$ from Eq. (1) for the case when solidification rate changes in accordance with the law depicted in Fig. 7*b*. It is apparent that in accordance with the previous discussions on the impurity distribution in the vertical direction along the ingot axis, the concentration of impurities in the horizontal direction should initially decrease sharply going away from the ingot surface and then remain almost constant. However, it has been shown that this does not actually take place. As the distance from the surface of the ingot increases, impurity content in the radial direction decreases in the bottom part of the ingot, varies in behavior in the middle part, and increases in the part under the hot top. This discrepancy is probably related to the additional accumulation of impurities in the melt as a result of its displacement when the lower-lying layers of metal solidify. It should be noted that the descending path of the experimental curve which describes the change in impurity content is reflective specifically of the bottom part of the ingot, where the quantity of impurities forced into the melt as these layers solidify is minimal.

Thus, we have examined aspects of the distribution of segregates in ingots in the axial and radial directions. Available empirical data was used as an example to describe general tendencies regarding the change in the profile of impurity content in the longitudinal and transverse planes of an ingot. However, we did not consider certain unusual features of the segregate distribution. For example, we did not take into account that the curves which describe the distribution of impurities over the height and radius of an ingot have local extrema in certain cases (see Fig. 3*a*). These extrema are related to the fact that portions of the melt which have a high content of impurities cannot be moved into the region under the hot top and are thus caught in the body of the ingot. However, while such capture takes place at the microscopic level in the radial direction and depends on parameters of the ingot's dendritic structure – specifically, the rate of heat removal and the composition of the metal being cast – the presence of peaks on the distribution curve in the vertical direction is related to the capture of macroscopic volumes of the melt. The possibility of such capture taking place depends on the shape of the liquid metal bath, which is in turn determined by the geometry of the ingot.

When the distribution curves contain such peaks, the difference between the impurity contents of the surface zone and axial zone of the ingot will be smaller than in the absence of peaks because captured impurities will not be forced into axial zone. Thus, the impurity content of that zone will remain lower than it would otherwise.

It should be emphasized that one direct consequence of having segregates captured in the spaces between dendrites is the formation of nonaxial stringers. Thus, the position of the segregate-concentration peaks on macroscopic metallographic sections can be determined based on the location of the stringers. The thermophysical conditions needed for the formation of large isolated dendritic cells were discussed in [1]. The presence of such cells can lead to stringer formation and raise the concentration of segregates over the radius of the ingot to extremely high values.

The validity of the above explanation for the formation of concentration peaks on curves that describe the distribution of impurities over the height of the axial part of ingots can be established from an analysis of experimental data on the chemical heterogeneity of ingots. Figure 9 shows results obtained from analyzing the carbon distribution over the height of the axial part of ingots weighing 360 and 142 tons. It is apparent from the data that there are a large number of local extrema on the curve for the 360-ton ingot, while the curve of carbon distribution over the height of the 142-ton ingot is relatively smooth.

The method in [13] was used to evaluate the geometry of these ingots from the standpoint of satisfaction of the conditions necessary for directional solidification. The evaluation showed that those conditions were satisfied in the 142-ton ingot but were not in the 360-ton ingot. This confirms the results of the computer modeling (the dark regions in the axial part of the ingots in Fig. 9), which showed that the 142-ton ingot was free of axial porosity (an ingot defect that develops when the conditions necessary for directional solidification are not present) but the 360-ton ingot was not. The size of the region affected by axial porosity was in fact quite large in the latter ingot.

Thus, the experimental data confirm the existence of impurity concentration peaks on the axial distribution curve of ingots whose geometry does not satisfy the prerequisites for directional solidification (see Fig. 9).

It should be pointed out that although the conditions needed for directional solidification were present in the 142-ton ingot (no data was obtained on the radial impurity distribution in the 360-ton ingot), due to the ingot's large transverse dimensions the dendritic structure that was formed during solidification turned out to be large enough to capture the segregate-rich liquid in the spaces between the dendrites. This ultimately led to the formation of stringers and segregate concentration peaks on the radial distribution curve (see Fig. 3*a*).

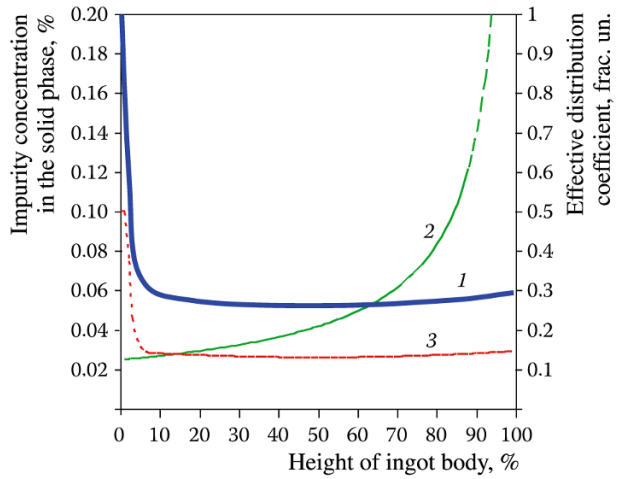

Fig. 8. Change in the effective distribution coefficient (*1*) and concentration of impurities over the radius of the ingot with a constant distribution coefficient (*2*) and a distribution coefficient that depends on the content of the solid phase (*3*).

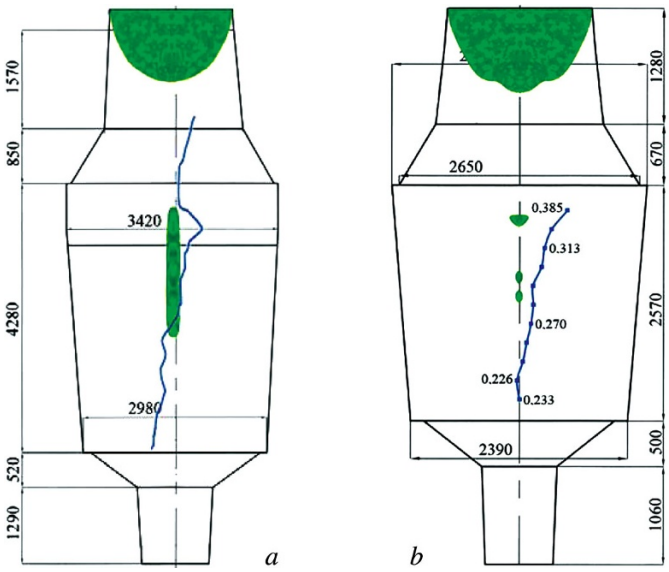

Fig. 9. Geometric dimensions and chemical and physical nonuniformity of 360-ton ingot of steel 25Kh2NMFA [11, 12] (*a*) and 142-ton ingot of steel 25KhN3MFA [1] (*b*); the points next to the curves represent the concentration of carbon, %; the dark regions in the axial part of the ingot represent sections characterized by axial porosity.

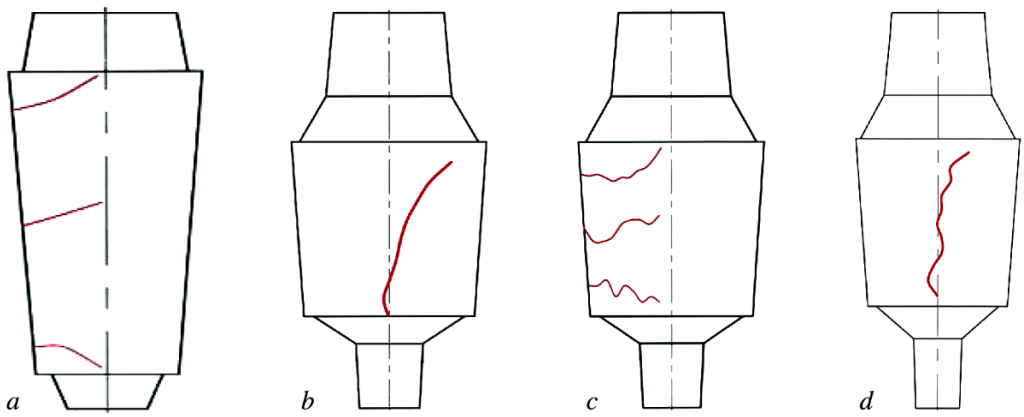

Fig. 10. Typical distribution of segregates in the radial (*a*, *c*) and axial (*b*, *d*) directions of forging ingots: *a*) radial distribution of impurity concentration in ingots without nonaxial stringers; *b*) axial distribution of segregates in ingots without axial porosity; *c*) radial distribution of impurity concentration in ingots damaged by nonaxial stringers; *d*) axial distribution of segregates in ingots damaged by axial porosity.

Thus, qualitative analysis of the chemical heterogeneity of forging ingots has shown that in ingots which do not have a region occupied by nonaxial stringers the concentration of segregates in the radial direction decreases in the bottom part of the ingot, increases under the hot top, and varies in the middle part (depending on the number of impurities that have accumulated in the liquid during previous stages of the solidification process) (Fig. 10*a*). In the axial direction, segregate distribution over the height of the axial zone of ingots in which conditions are favorable for directional solidification decreases up to the height of (0.2–0.3)*H* and then increases (Fig. 10*b*).

If conditions that are favorable to the formation of nonaxial stringers develop in an ingot during its solidification, concentration peaks will appear on the radial distribution curves and the coordinates of the peaks will coincide with the locations of the stringers (Fig. 10*c*). Similar peaks will appear on curves showing the impurity distribution in the axial part of ingots if their geometry does not facilitate directional solidification (Fig. 10*d*).

Conclusions. An analysis was made of literature data on the chemical heterogeneity of forging ingots and general patterns were identified in regard to the distribution of segregates in these ingots in the vertical and horizontal directions.

It was shown that impurity concentration in the axial direction usually first decreases up to a height of roughly 0.25*H* above the bottom of the ingot. It then begins to increase monotonically above this point.

Impurity concentration in the radial direction, from the periphery to the center, decreases in the bottom part of the ingot, is variable in the middle part, and increases substantially in the section under the hot top; here, the impurity content of the surface layers of the ingot usually increases slightly (by 10–15 rel.%) from its bottom to its top.

Substantiation was provided for possible explanations of the reasons for the above-described distribution of impurities in forging ingots.

REFERENCES

1. V. D. Dub, *Investigation of Nonaxial Segregation and Development of Methods of Suppressing It in Forging Ingots: Eng. Sci. Doct. Dissert.*, Moscow, TsNIITMASh (1980), Vol. 1.
2. I. I. Makarov, *Investigation of the Effect of the Parameters of Hot Tops on the Kinetics of Solidification of Steel and the Formation of Shrinkage Defects in Large Ingots: Eng. Sci. Doct. Dissert.*, Moscow, TsNIITMASh (1976).
3. N. D. Ageev, *Study of Steelmaking Conditions and the Casting, Structure, and Properties of Large Ingots*, TsNIITMASh Report, Moscow (1952).
4. A. P. Fomenko, *Design and Study of a Small-Hot-Top Ingot with Conical Walls to Produce Rolled Sections: Eng. Sci. Cand. Dissert.*, TsNIIchermet, Moscow (2007).
5. A. V. Mozgovoi, *Optimization of the Parameters of a Steel Ingot with Improved Axial-Zone Characteristics for the Production of Large-Diameter Rolled Sections: Eng. Sci. Cand. Dissert*., TsNIIchermet, Moscow (2009).
6. K. Nishiguchi, K. Nakanishi, K. Nakayama, et al., "Prediction on macro segregation in large forging ingots," *13th Int. Forgemasters Meeting, IFM 1997*, Oct. 12–16, 1997, Pusan, Korea, pp. 57–70.
7. E. Sheil, "Bemerkungen zur schicht kristallbildung," *Zeitschrift für Metallkunde*, **34**, No. 3, 70–72 (1942).
8. J. A. Burton, R. C. Prim, and W. P. Clichter, *J. Chem. Phys*., **33**, 723 (1955).
9. Y. Yamamoto, H. Muto, Y. Akimoto, et al., "Solidification analysis of mod. 9Cr–1 Mo steel," *17th Int. Forgemasters Meeting, IFM 2008*, Nov. 3–7, 2008, Santander, Spain.
10. K. Tashiro, Sh. Watanabe, I. Tamura, et al. "Influence of mold design on the solidification soundness of heavy forging ingot," *Transactions ISIJ*, **23**, 312–321 (1983).
11. V. S. Dub, E. V. Makarycheva, and I. I. Makarov, "The forging ingot – present and future," *Elektrometallurgiya*, No. 5, 22–30 (1999).
12. V. A. Durynin and Yu. P. Solntsev, *Study and Improvement of the Manufacturing Technology to Increase the Service Life of High-Priority Products Made from Large Forgings* [in Russian], Khimizdat, St. Petersburg (2006).
13. V. V. Nazaratin, A. N. Romashkin, I. A. Ivanov, et al., "Method of designing forging ingots without axial shrinkage defects," *Metall. Mashinostr.*, No. 3, 40–52 (2010).